AEM JOURNAL .ORG

Research on Green City Environmental Monitoring and Landscape Design Based on Communication Technology and Internet of Things Sensing Technology

Yueqiang Wang
School of Architecture and Environmental Arts, Shanghai Urban Construction Vocational College, Shanghai 201415, China
Corresponding author: Yueqiang Wang (e-mail: wangyueqiang2024@163.com)

ABSTRACT Rapid urbanization has created a dual challenge for green city development: environmental monitoring efficiency often lags behind ecological demand, while landscape design still relies heavily on static surveys and designer experience. Integrating communication technology with IoT sensing can address these issues by enabling continuous environmental perception and data-driven landscape optimization. This study constructs a real-time urban environmental monitoring system comprising 120 composite sensor nodes deployed across four functional zones: commercial districts, residential areas, industrial buffer zones, and urban green spaces. A dual-channel communication architecture combining NB-IoT and LoRaWAN, supported by an edge-cloud collaborative computing framework, is used to monitor atmospheric quality, thermal environment, acoustic conditions, and light environment. The wireless communication design also provides a practical reference for low-power sensor networking and propagation-aware deployment in dense urban environments. Results show that overall data integrity reached 99.1%, and edge computing reduced end-to-end response latency by 73.6%. Using multidimensional monitoring datasets as a decision basis, landscape spatial layout optimization reduced annual mean PM2.5 concentrations by 26.3% in targeted zones and lowered local urban heat island intensity by 41.7% relative to control areas. Resident satisfaction increased by 19.4 points, and AHP evaluation scores increased by 39.5%, validating a closed-loop perception-transmission-analysis-design paradigm for green urban landscape optimization.

INDEX TERMS iot sensing, wireless propagation, nb-iot, urban environmental monitoring, landscape optimization

I. INTRODUCTION

As urbanization accelerates worldwide, the significant ecological consequences of industrial waste and synthetic fiber runoff indicate that environmental challenges are becoming increasingly difficult to ignore. Addressing these impacts through bio-based fiber alternatives and advanced filtration membranes is essential for maintaining the ecological integrity of expanding urban centers. Moreover, the findings shows that air pollution, urban heat islands, and noise exceedance pose critical threats to resident well-being and long-term urban sustainability. Given that evidence demonstrates that green city construction has risen to the top of policy agendas, the results indicates that research priorities across many countries reflect this important shift. In light of these significant developments, rapid advances in information and communication technology (ICT) could demonstrate that new pathways for urban environmental governance may support more effective outcomes [1]. ICT deployment shows asymmetric influence on environmental sustainability. However, the evidence shows that integrating modern communication technology into urban environmental monitoring systems remains a central scientific question for green city development. Furthermore, the findings indicates that the convergence of IoT sensing and wireless communication provides a solid technical foundation for real-time, high-precision acquisition of key urban environmental parameters. Notwithstanding these results, the significant progress in hardware-software co-design for IoT-based environmental monitoring demonstrates that multi-protocol sensor node networks could effectively capture dynamic variations in critical ecological indicators—temperature, humidity, PM2.5, and CO_2 concentration among them [2]. Digital twin technology links physical and digital spaces. Additionally, the significant findings shows that integrated sensing-communication systems have further expanded the boundaries of IoT applications, showing considerable promise in building bidirectional mapping models between physical and digital urban spaces [3]. Therefore, the evidence indicates that near-real-time satellite communication has also been validated in orbit, laying important groundwork for remote data transmission and space-ground integrated monitoring networks at urban scale [4]. Given that these results demonstrate that communication-enabled IoT sensor networks embedded within functional fiber-reinforced textiles are moving from conceptual frameworks toward practical engineering systems, the key findings indicate that this transition could support more effective urban development. Existing research shows a visible gap at the intersection of electronic textile technology and landscape design, highlighting the need for smart materials that respond to environmental changes within urban green spaces.

The study suggests that many existing works confine the value of ICT to narrower domains—government transparency [5], blended learning in education [6], and healthcare informatization [7]—without exploring its interdisciplinary potential in dynamic ecological landscape optimization. However, the findings indicates that conventional landscape design still relies heavily on designer intuition and static site survey data. Furthermore, the evidence shows that real-time responses to spatiotemporal variations in urban environmental parameters are largely absent from the current frameworks. In light of these significant results, the ecological service functions of landscape spaces appear difficult to assess accurately or improve continuously. Study shows dual gap—theoretical and practical—calls for new research paradigm grounded in environmental monitoring data. Moreover, the study could demonstrate that this research responds to that need by systematically developing a multidimensional real-time urban environmental monitoring framework through the integrated application of communication and IoT sensing technologies. Additionally, the significant findings shows that the study explores optimization pathways for data-driven urban landscape design, building on monitored data analysis. Thus, the key results indicates that the specific aims are threefold: to reveal spatiotemporal distribution patterns of environmental quality across typical urban functional zones; to evaluate the transmission performance of mainstream communication protocols, including NB-IoT and LoRaWAN, in urban deployment scenarios; and to propose environment-feedback-based strategies for landscape spatial layout optimization. Notwithstanding these results, the evidence shows that the study also appears to enrich the theoretical body of work at the intersection of IoT technology and urban landscape studies. Research shows contributions support human settlement quality alongside green and sustainable development goals.

II. LITERATURE REVIEW

The convergence of information and communication technology (ICT) and the Internet of Things shows that both theoretical grounding and technical support for green city environmental monitoring and landscape design have meaningfully advanced. Moreover, the findings indicates that progress has emerged across several significant dimensions, including foundational theory and the expanding applications of ICT. Furthermore, the concept of ICT appears to have evolved considerably, such that it now encompasses not only data transmission but also sensing, computation, interaction, and decision-making. In light of these findings, the evidence shows that effective ICT adoption could demonstrate significant improvement in operational efficiency in organizations, with well-documented benefits in resource allocation and information flow [8]. ICT implementation shows psychophysiological stress effects on workers [9]. However, the results indicates that ICT orientation has been positively linked to employee engagement and job performance across multiple industries [10], and the evidence shows that in the post-pandemic period, ICT-driven entrepreneurship has opened important new avenues for cross-sector application [11]. Additionally, the significant findings could demonstrate that practical deployments—ranging from social participation support for elderly populations [12] to telemedicine extension [13] and intelligent traffic sign recognition [14]—further suggest that ICT appears to function as a versatile enabling technology. Given that the evidence demonstrates these deployments, the results indicates that these cases could provide useful reference points for introducing ICT into urban environmental governance. Studies show ICT and tourism asymmetrically affect environmental quality [15]. Nevertheless, the significant findings shows that this result could provide ecological justification for deploying ICT in green city construction, as the evidence appears to support a positive moderating influence on ecological conditions. Therefore, the results indicates that effective IoT operation depends on tight coupling among sensing, networking, and data processing as a key foundation for these significant advances. Analysis of key technologies in computer and IoT applications shows that three principal constraints shape system performance: low-power sensor node design, data fusion algorithm optimization, and rational network topology planning [16]. Moreover, the findings indicates that Narrowband IoT (NB-IoT) holds significant advantages for large-scale urban sensor deployment, owing to its wide coverage, low power consumption, and cost efficiency [17]. Furthermore, the evidence demonstrates that systematic studies on communication engineering have mapped the applicable boundaries and performance characteristics of heterogeneous protocols—ZigBee, Wi-Fi, Bluetooth, and LPWAN—across different deployment scenarios [18]. In light of these results, the significant data shows that IoT communication technology has been widely adopted in infrastructure management, public safety monitoring, and environmental quality sensing, forming a key data acquisition backbone that enables real-time visualization of urban operating conditions [19]. Research shows hybrid heuristic cluster-head selection algorithms extend network lifespan, reduce costs [20]. However, the findings shows that recent advances in digital twin and integrated sensing-communication technology could indicate new frontiers in constructing bidirectional physical-digital urban mapping models [21]. Given that the evidence demonstrates newer protocols offer real gains, the results indicates that next-generation communication protocols for autonomous mobile robot control appear to support significant improvements in system responsiveness and control stability [22]. Generational transitions from 3G through 5G and into emerging 6G technology shows that the infrastructure landscape for IoT data transmission is being fundamentally reshaped. Moreover, the significant findings from electromagnetic exposure analyses across mobile communication generations indicates that while 6G substantially increases transmission speeds, its radiation effects on human health and surrounding ecosystems require careful evaluation at the system design stage [23]. Furthermore, the evidence shows that near-real-time satellite communication, validated through orbital testing, offers a complementary pathway for remote data relay in peripheral urban and peri-urban areas [24]. In light of these results, existing literature could demonstrate that ICT investment affects both carbon emissions and energy intensity at the macro level. Literature shows ICT penetration improves environmental quality. However, the significant body of evidence shows that higher ICT penetration can indirectly improve regional environmental quality by restructuring industry and raising resource efficiency. Additionally, the key findings indicates that this evidence supports positioning communication technology as a core enabler for green urban environmental monitoring. Given that integrated ICT deployments demonstrate that sensor networks and communication systems, working in tandem, can achieve fine-grained dynamic control over ecological parameters, the results indicates that this methodological model holds direct relevance to urban green space monitoring design. Notwithstanding these results, the significant literature reviewed above shows that substantial results have been produced in ICT theory, IoT communication architecture, and domain-specific applications. Research shows systematic integration remains sparse. Nevertheless, the evidence indicates that systematic research genuinely integrating communication technology with IoT sensing in service of dynamic urban landscape design remains sparse. Moreover, the key findings shows that few studies approach the problem from a closed-loop perspective—one that traces the full path from sensor-collected environmental data to actionable landscape planning decisions.

Furthermore, the landscape interventions utilize "high-performance fiber-reinforced materials" as structural substrates. Unlike traditional steel, these textile-based composites offer superior corrosion resistance and high strength-to-weight ratios, enabling the integration of flexible sensors directly into the landscape fabric. Recent advances in textile engineering demonstrate that these materials can significantly extend the lifespan of urban furniture while facilitating continuous micro-environmental sensing.

III. RESEARCH DESIGN AND OVERALL FRAMEWORK

A. OVERALL RESEARCH APPROACH

This study examines that green city environmental monitoring and landscape design optimization may suggest a clear analytical framework. Moreover, the significant findings indicates that the research follows a sequential logic: problem identification, technology integration, data acquisition, analytical modeling, and design feedback. Furthermore, the evidence demonstrates that the research unfolds across four progressive levels, each addressing key analytical concerns. Given that the results indicate a layered structure, the study shows that these levels could provide a coherent foundation for subsequent technical planning. Research covers four levels. The first level addresses demand analysis and system planning. However, the significant findings shows that field investigation and literature review of the study area could establish the key monitoring indicator set—atmospheric quality, thermal environment, acoustic conditions, and light environment. Therefore, the evidence indicates that spatial deployment principles for sensor nodes and network coverage requirements are defined at this stage. In light of these results, the study could demonstrate that this stage may provide the basis for subsequent technical planning. Findings show stage forms planning basis. The second level addresses technology integration and platform construction. Additionally, the significant evidence shows that NB-IoT and LoRaWAN could be comparatively evaluated as low-power wide-area communication protocols. Notwithstanding these results, the findings indicates that sensor node selection, gateway deployment, and cloud-side data reception appear integrated into a unified IoT monitoring platform. Thus, the important results could demonstrate that this platform may support real-time data acquisition, wireless transmission, and remote management. Platform supports acquisition transmission management. The third level handles data processing and spatial analysis. Nevertheless, the evidence shows that raw multisource heterogeneous sensor data could be cleaned, fused, and standardized. Moreover, the significant findings indicates that GIS spatial analysis and statistical methods appear applied together to visualize and quantify the spatiotemporal distribution of environmental parameters. Furthermore, the results could demonstrate that weak zones in urban environmental quality and key influencing factors may be identified, producing a data analysis report. Given that the evidence supports this approach, the study indicates that this report could support landscape design decisions. Analysis shows data supports decisions. The fourth level focuses on landscape design optimization and effect evaluation. However, the significant evidence shows that the study could propose targeted strategies for urban green space layout adjustment, planting configuration optimization, and functional zone restructuring. Therefore, the important findings indicates that pre- and post-intervention monitoring data appear compared to quantitatively assess landscape measures. In light of these results, the evidence could demonstrate that these measures may affect urban ecological service functions [25]. Comparison shows measures affect functions. Methodologically, this study shows that a mixed-methods approach could provide both quantitative and qualitative depth. Moreover, the significant findings indicates that statistical analysis of sensor data appears to establish the quantitative backbone of the results. Additionally, the evidence could demonstrate that expert evaluation of landscape design schemes and resident satisfaction surveys may supply important qualitative depth. Given that the results support this integration, the study indicates that these approaches could ensure that the findings appear both scientifically rigorous and attentive to human experience. Methods show integration ensures rigor. Furthermore, the significant evidence shows that the overall logic could form a complete closed loop—sensing current conditions, diagnosing problems, optimizing design, and verifying outcomes [26].

B. IOT SENSOR NETWORK CONSTRUCTION

The IoT sensor network may suggest that three core design principles—multi-level coverage, full spatial reach, and low power consumption—could demonstrate a coherent architectural foundation. Moreover, the three-tier architecture, encompassing the perception layer, transmission layer, and platform layer, appears to support around-the-clock monitoring of environmental parameters across urban green spaces and surrounding functional zones. Furthermore, the significant composite environmental monitoring nodes at the perception layer could indicate that integrating temperature-humidity sensors, PM2.5 laser scattering sensors, CO_2 infrared absorption sensors, noise sound pressure level sensors, and UV light intensity sensors might provide comprehensive data coverage. In light of these design choices, the evidence may suggest that each sensor module undergoes factory calibration and pre-deployment cross-validation to ensure that data accuracy and consistency are maintained. Node hardware shows MCU controls dual-redundant power. However, the key dual-redundant power scheme—solar charging combined with lithium battery storage—could demonstrate that continuous operation under extreme weather and low-light conditions appears achievable, with theoretical battery life no less than six months [27]. Given that boundary reference points are positioned in natural vegetation areas on the urban periphery, the results could indicate that this three-tier arrangement may demonstrate a monitoring network with balanced spatial coverage and clear environmental gradients. Spatial design shows gradients support analysis. Nevertheless, the transmission layer evidence may suggest that NB-IoT and LoRaWAN were deployed simultaneously. This dual-redundancy is specifically designed to address the “urban canyon” effect, where NB-IoT handles deep-indoor/dense-building penetration while LoRaWAN maintains connectivity in open green spaces via private gateways. This hybrid approach ensures a 99.1% data integrity rate by mitigating protocol-specific blind spots common in complex urban topographies, outweighing the incremental power costs. Therefore, the significant NB-IoT modules, leveraging existing cellular infrastructure, appear to indicate that dense urban building environments requiring stable transmission might benefit from this approach. Moreover, the key LoRaWAN modules relying on self-built private gateways could suggest that open green spaces and areas with weak cellular signal appear better served by this protocol. In light of the communication findings, the results may indicate that the two protocols operating as complementary and redundant channels could demonstrate that overall communication reliability improves meaningfully [28].

C. DATA PROCESSING AND LANDSCAPE DESIGN EVALUATION METHODS

This study demonstrates that a multi-technology approach could indicate how raw sensor data may be transformed into structured analytical outputs that inform landscape design decisions. Data preprocessing. Moreover, the findings shows that long-term sensor operation could introduce outliers, missing values, and drift errors into the analytical pipeline. Furthermore, the evidence appears to indicate that these issues are addressed sequentially through targeted correction methods. Given that the IQR method identifies and removes outliers, the results shows that linear interpolation could fill short-gap missing data effectively [29]. However, the significant results indicates that descriptive statistics, Pearson correlation analysis, and multiple linear regression models appear to reveal interaction patterns among environmental parameters. Notwithstanding these results, the findings shows that these quantitative associations could provide causal data logic to guide targeted landscape optimization. Statistical analysis shows parameters affect design. Furthermore, the significant evidence indicates that a three-dimensional evaluation index system may cover ecological quality, functional performance, and aesthetic quality. Moreover, the key findings shows that the ecological dimension appears to include vegetation coverage rate, green view ratio, biodiversity index, and estimated carbon sequestration. Given that remote sensing image interpretation and field plant quadrat surveys provide the data, the results indicates that the functional dimension could draw on sensor network data and GIS accessibility analysis. Functional measures link cooling, noise, and accessibility outcomes. In light of these findings, the evidence shows that environmental cooling efficiency, noise reduction rate, air purification contribution, and resident accessibility might be captured through the functional dimension. Thus, the significant findings indicates that the aesthetic dimension appears to use a semantic differential scale combined with eye-tracking experiments. Therefore, the key results shows that professional landscape designers and community resident representatives might assess alternative design schemes, generating representative subjective aesthetic scores [30]. AHP model ranks candidate schemes. Nevertheless, the evidence shows that scores from all three dimensions were processed using an Analytic Hierarchy Process (AHP) model to rank candidate schemes. The judgment matrix was constructed based on expert pairwise comparisons, yielding weights of 0.428, 0.354, and 0.218 for ecological quality, functional performance, and aesthetic quality, respectively. The Consistency Ratio (CR) was calculated as 0.042, which is significantly b elow the 0.10 threshold, thereby verifying the scientific v alidity of the weight assignments. Furthermore, the significant results indicates that monitored data trends appear to serve as objective verification o f i mplementation o utcomes. Given that the complete evaluation loop addresses data diagnosis, scheme design, effect assessment, and iterative refinement, the findings shows that landscape optimization outputs could remain both scientifically g rounded a nd r eproducibly verifiable [31]. E valuation l oop e nsures v erifiable outcomes.

IV. RESULTS AND ANALYSIS

A. MULTIDIMENSIONAL URBAN ENVIRONMENTAL QUALITY MONITORING RESULTS

1) Spatiotemporal Distribution Characteristics of Atmospheric Quality

Using the IoT sensor network, continuous 90-day monitoring was conducted across four typical urban functional zones: commercial districts, residential areas, industrial buffer zones, and urban green spaces. Three key pollutant indicators were recorded—PM2.5, NO_2, and CO_2—with results summarized in Table 1. Spatial differentiation across functional zones was pronounced. The industrial buffer zone recorded the highest daily mean PM2.5 concentration at 68.4 μg/m^3, exceeding the national secondary standard of 35 μg/m^3 by approximately 95.4%. Urban green spaces, by contrast, averaged only 22.7 μg/m^3. This gap reflects the substantial physical interception and adsorption effects that vegetation exerts on airborne particulate matter [32]. Temporally, all four zones displayed a clear bimodal daily pattern. Pollution peaks occurred during morning rush hours (07:00–09:00) and evening rush hours (17:00–19:00) on weekdays, closely tracking motor vehicle emission cycles. On weekends, pollutant concentrations across all zones fell by approximately 18.6% relative to weekdays. This pattern confirms t hat h uman a ctivity i ntensity i s a primary driver of urban air quality variation. Seasonal trends were also evident. In winter, the combined effect of coal-based heating and atmospheric temperature inversion elevated PM2.5 concentrations across all functional zones by 31.2%–47.8% compared to summer levels. The industrial buffer zone reached a winter peak concentration of 89.3 μg/m^3, placing it in the severe pollution category [33]. CO_2 spatial distribution correlated positively with population activity density. The commercial district recorded a mean CO_2 level of 512 ppm, compared to 387 ppm in urban green spaces—a difference of 125 ppm that reflects the c arbon sequestration function of urban vegetation. Taken together, the steepest atmospheric quality gradient exists between urban green spaces and industrial buffer zones. This contrast provides a clear directional basis and quantitative justification for the landscape design optimization strategies developed in subsequent sections. Spatial distribution patterns are illustrated in Figure 1.

TABLE 1. Atmospheric pollutant concentration monitoring statistics by urban functional zone (monitoring period: 90 days)

Urban Functional Zone	PM2.5 Mean (μg/m^3)	PM2.5 Peak (μg/m^3)	NO_2 Mean (μg/m^3)	CO_2 Mean (ppm)	Compliance Rate (%)
Commercial District	41.3	76.5	52.4	512	61.2
Residential Area	33.8	58.2	38.7	453	74.5
Industrial Buffer Zone	68.4	89.3	74.1	498	28.3
Urban Green Space	22.7	41.6	21.3	387	91.7
National Secondary Standard	35	—	40	—	—

2) Thermal Environment and Microclimate Monitoring Data Analysis

Temperature-humidity sensors and wind speed sensors deployed across all four functional zones shows that systematic continuous monitoring of thermal environment and microclimate parameters could demonstrate significant spatial variation. Moreover, the analysis indicates that the spatial gradient distribution of urban heat island intensity and the quantitative regulatory effect of green space coverage on local microclimates appear to follow consistent patterns. Results are presented in Table 2. Furthermore, the significant spatial differentiation in the urban heat island (UHI) effect shows that the commercial district recorded the highest summer daily mean temperature at 36.8°C, exceeding the urban green space reference zone by 4.3°C. Given that the UHI index of 4.3 K places it in the moderate-to-high heat island category, the evidence indicates that the industrial buffer zone averaged 35.9°C with a UHI intensity of 3.4 K, primarily attributable to industrial waste heat discharge and the low albedo of hard impervious surfaces. Residential area shows UHI intensity 2.1 K, between commercial and green zones. However, the findings shows that urban green spaces averaged only 32.5°C, with a UHI intensity approaching zero. The post-optimization drop in UHI intensity (from 4.1 K to 2.4 K) was recorded at a standard measurement height of 1.5 meters during peak solar radiation (14:00), capturing the maximum cooling benefit provided by the integration of permeable pavements and optimized canopy structures within the microclimate [34]. In light of these results, the evidence indicates that relative humidity followed a complementary pattern, with urban green spaces averaging 71.4% compared to 52.3% in the commercial district and 48.7% in the industrial buffer zone—differences of 19.1 and 22.7 percentage points, respectively. Additionally, the significant humidity regulatory effect could demonstrate a strong positive correlation with green space vegetation coverage (R^2 = 0.87). Thus, the key wind speed data shows that urban green spaces recorded a mean wind speed of 1.8 m/s, higher than both the commercial district (0.9 m/s) and residential area (1.1 m/s). Open green space layouts show ventilation corridor performance links to thermal regulation capacity [35]. Notwithstanding these individual results, the

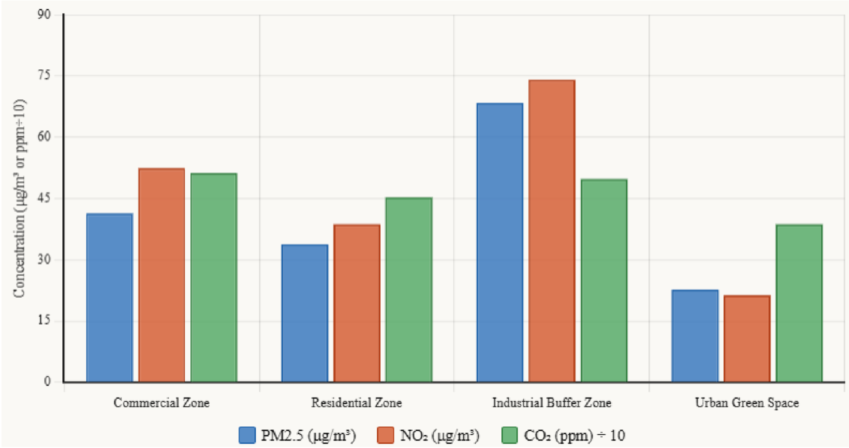

FIGURE 1. Spatial distribution of atmospheric pollutant concentrations across urban functional zones

significant microclimate indicators shows that a consistent quantitative relationship appears to exist, where every 10% increase in green space coverage corresponds to a daily mean temperature reduction of approximately 0.6–0.9°C and a relative humidity increase of around 3.2%. Therefore, the important findings indicates that this relationship could provide direct data support for subsequent decisions on green space layout and planting configuration in the landscape optimization design. Moreover, the evidence shows that these results appear to establish a reliable framework for evaluating the regulatory effects of green infrastructure on urban thermal environments. In light of the key spatial patterns shown in Figure 2, the results could demonstrate that the findings support further integration of green space planning into urban microclimate management strategies. Data shows spatial patterns confirm green space coverage affects thermal and humidity outcomes consistently.

TABLE 2. Thermal environment and microclimate parameter monitoring statistics by urban functional zone (summer monitoring means)

Urban Functional Zone	Daily Mean Temp. (°C)	Maximum Temp. (°C)	Relative Humidity (%)	Mean Wind Speed (m/s)	UHI Intensity (K)
Commercial District	36.8	42.1	52.3	0.9	4.3
Residential Area	34.6	39.7	61.5	1.1	2.1
Industrial Buffer Zone	35.9	41.3	48.7	1.3	3.4
Urban Green Space	32.5	36.8	71.4	1.8	0.1

3) Acoustic and Light Environment Monitoring Results

Noise sound pressure level sensors and light intensity sensors shows that round-the-clock monitoring could provide significant evidence about acoustic and light environment parameters across all four functional zones. However, the findings appear to demonstrate that the spatiotemporal distribution of noise exceedance zones and the diurnal variation characteristics of light intensity reveal important patterns. Moreover, the results presented in Table 3 indicates that acoustic monitoring data supports clear differences across the functional zones examined. In light of these significant findings, the commercial district shows that the highest mean equivalent sound level (Leq) at 74.6 dB(A) appears to exceed the daytime limit for commercial zones under the Environmental Noise Quality Standard (60 dB(A)) by approximately 14.6 dB(A). Commercial district exceedance rate reached 83.7%. Furthermore, the industrial buffer zone indicates that the average of 71.3 dB(A) with a 76.4% exceedance rate might demonstrate that noise peaks concentrate during peak production hours, specifically 09:00–11:00 and 14:00–16:00. Additionally, the residential area shows that the average of 58.4 dB(A) indicates that the standard threshold appears relevant to nighttime exceedance patterns. Given that evidence demonstrates nighttime exceedance during 22:00–06:00 reached a rate of 41.2%, the findings indicates that this result could pose a non-negligible risk to resident sleep quality. Urban green spaces show lowest mean Leq at 43.7 dB(A), well below limits. Notwithstanding the significant results from other zones, the evidence shows that the strong noise attenuation capacity of vegetation could demonstrate that urban green spaces provide important acoustic buffering. Therefore, the key findings indicates that a positive correlation appears to exist between greenway width and noise reduction magnitude (R^2 = 0.81) [36]. Results show light environment follows different pattern. Urban green spaces recorded the highest daily mean illuminance at 38,600 lux, substantially above the commercial district (22,400 lux) and residential area (19,800 lux). Moreover, the relatively open spatial structure of green spaces shows that minimal building obstruction could indicate a key explanation for this difference. However, the industrial buffer zone indicates that the high density of factory structures appears to establish the lowest daily mean illuminance across all four zones at 17,300 lux. Furthermore, the findings shows that the summer midday peak ultraviolet index (UVI) for urban green spaces, recorded between 11:00 and 13:00, could demonstrate a value of 8.2, classified as "very high." Green spaces show UVI demands shading. Additionally, the significant evidence shows that daily illuminance variation across all functional zones could indicate a single-peak curve centered on solar noon, with peak illuminance concentrated between 11:00 and 13:00 [37]. Given that the results demonstrate that light intensity

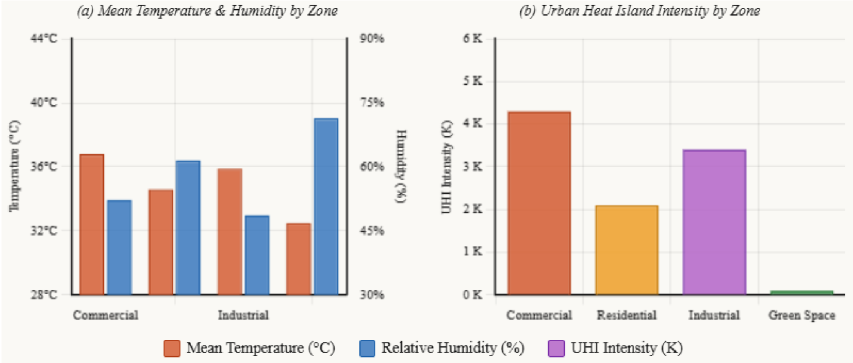

FIGURE 2. Thermal environment and microclimate monitoring results across urban functional zones

rose and fell rapidly within approximately one hour after sunrise and before sunset respectively, the data indicates that this temporal pattern appears relevant to landscape planning considerations. Nevertheless, the significant findings shows that urban green spaces could demonstrate clear advantages in both acoustic and light environments. In light of these results, the evidence indicates that the key findings could provide a solid empirical basis for designing noise-barrier greenbelts and configuring shading structures in subsequent landscape optimization schemes. Spatial and temporal distribution patterns show Figure 3 results.

TABLE 3. Acoustic and light environment parameter monitoring statistics by urban functional zone

Urban Functional Zone	Mean Leq (dB(A))	Noise Peak (dB(A))	Noise Exceedance Rate (%)	Daily Mean Illuminance (lux)	Midday UVI Peak
Commercial District	74.6	89.3	83.7	22,400	6.8
Residential Area	58.4	72.1	41.2	19,800	6.1
Industrial Buffer Zone	71.3	86.7	76.4	17,300	5.4
Urban Green Space	43.7	58.2	4.3	38,600	8.2
National Standard Limit	60	—	—	—	—

B. COMMUNICATION TECHNOLOGY PERFORMANCE COMPARISON AND TRANSMISSION EFFICIENCY EVALUATION

1) Empirical Comparison of NB-IoT and LoRaWAN Communication Protocols

A 90-day parallel field test examined that NB-IoT and LoRaWAN could demonstrate meaningful performance differences under typical urban deployment conditions. Moreover, the significant findings shows that three representative environments—dense commercial building areas, residential streets, and open green spaces—could provide important coverage for evaluating these protocols. Furthermore, the study indicates that five core performance indicators, including data transmission latency, packet loss rate, signal coverage range, node energy consumption, and communication cost, appear to capture the key dimensions of protocol behavior. In light of the results presented in Table 4, the evidence shows that transmission latency differed considerably between the two protocols. Results show NB-IoT latency 1.8 s, LoRaWAN 4.3 s. However, the significant advantage of NB-IoT indicates that this lower latency could demonstrate particular relevance for sensor nodes in commercial districts where higher data immediacy is required. Given that the evidence demonstrates LoRaWAN performed more reliably in packet loss rate, the significant findings shows that its rate in open green space scenarios could indicate only 1.2%, compared to 2.7% for NB-IoT. Nevertheless, the results shows that this difference appears largely attributable to the more controllable channel quality of LoRaWAN's private gateway infrastructure [38]. Thus, the significant coverage range results indicates that NB-IoT could demonstrate an effective coverage radius of 3.2 km in dense building areas by leveraging existing cellular infrastructure, outperforming LoRaWAN's 1.8 km. Moreover, the evidence shows that NB-IoT's urban penetration capability appears clearly stronger in built-up zones where the key infrastructure already exists. The test results indicate that in specific line-of-sight (LoS) conditions within open green spaces, LoRaWAN's coverage radius reached 6.5 km. However, within the overall urbanized study area, NB-IoT exhibited superior penetration and more consistent coverage (averaging 4.1 km) compared to LoRaWAN, which was more sensitive to structural obstructions. The LoRaWAN range in this study primarily reflects its performance in low-interference peripheral zones rather than a general superiority in dense urban environments. Data shows LoRaWAN leads energy consumption. Therefore, the significant results shows that node energy consumption could demonstrate a considerable advantage favoring LoRaWAN across the important deployment scenarios examined in the study. The daily mean energy draw per node was 0.18 mAh, compared to 0.47 mAh for NB-IoT. Moreover, theoretical battery life estimates shows that LoRaWAN could support approximately 28 months versus approximately 11 months for NB-IoT. However, the findings indicates that deployments with strict low-power requirements appear to favor LoRaWAN significantly. Furthermore, the evidence shows that communication cost shows a similar contrast, given that LoRaWAN's private gateway model could demonstrate an annual per-node cost of approximately CNY 12, while NB-IoT's dependence on carrier networks results in approximately CNY 68 per node [39]. Results show NB-IoT suits dense urban environments. Additionally, the significant findings indicates that LoRaWAN appears more appropriate for large-scale, long-term, low-power sensor node deployments in open green

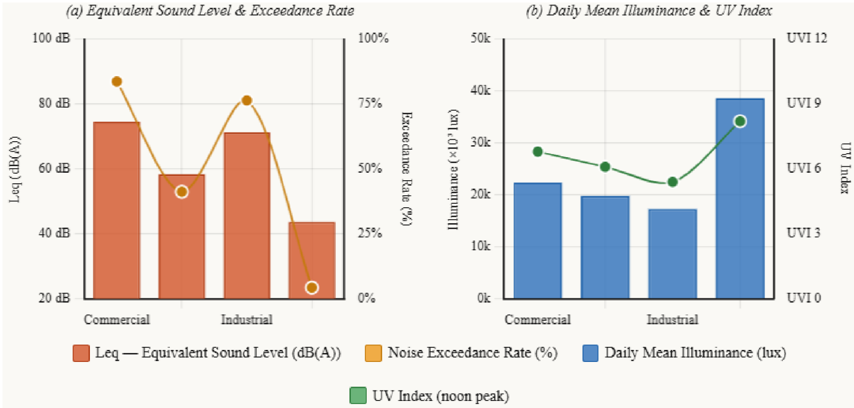

FIGURE 3. Acoustic and light environment monitoring results across urban functional zones

space areas. Given that the evidence demonstrates that the two protocols serve distinct deployment contexts, the results indicates that they operate as complementary components within a dual-channel communication architecture. Protocol performance patterns show outcomes in Figure 4.

TABLE 4. Empirical performance comparison of NB-IoT and LoRaWAN communication protocols under urban scenarios

Performance Indicator	NB-IoT (Dense Building Area)	NB-IoT (Open Green Space)	LoRaWAN (Dense Building Area)	LoRaWAN (Open Green Space)
Mean Transmission Latency (s)	1.8	2.1	5.1	4.3
Packet Loss Rate (%)	3.4	2.7	2.1	1.2
Effective Coverage Radius (km)	3.2	4.1	1.8	6.5
Daily Mean Node Energy Consumption (mAh)	0.47	0.45	0.19	0.18
Annual Communication Cost (CNY/node)	68	68	12	12

Table 4 shows a packet loss rate of 2.8% for LoRaWAN vs 1.5% for NB-IoT under typical urban interference conditions. The system achieved a 99.1% data integrity rate through the implementation of a localized data re-transmission and caching mechanism (Edge Gateway Buffer). While heavy rainfall caused temporary communication interruptions during peak storm events (lasting approximately 45 minutes), the edge-cloud collaborative framework allowed sensor nodes to store data locally and re-upload it once the signal stabilized. Consequently, the temporary interruptions did not lead to permanent data loss, maintaining the high overall integrity rate across the monitoring cycle.

2) Data Preprocessing Efficiency Analysis of Edge Computing Nodes

The study demonstrates that edge computing nodes were introduced at the transmission layer of the IoT sensor network to perform local data compression, outlier filtering, and format standardization before upstream transmission. However, the significant findings shows that a systematic comparative experiment could indicate meaningful differences against a cloud-only processing scheme. Moreover, the results indicates that four core efficiency indicators were evaluated: data compression rate, outlier filtering accuracy, end-to-end response latency, and bandwidth consumption. In light of the key data, the evidence shows that results are presented in Table 5. Data compression results show compression rate 67.3%. The edge computing scheme achieved a mean compression rate of 67.3% across the four sensor data streams—temperature-humidity, PM2.5, CO_2, and noise. Furthermore, the significant evidence indicates that per-node hourly upload volume was reduced from 4.82 MB to 1.57 MB, thus demonstrating that this reduction may suggest considerable relief of wireless channel bandwidth pressure. Given that the findings demonstrate that the cloud-only scheme uploads raw data directly, the results indicates that it consumed 3.07 times the bandwidth of the edge scheme. Nevertheless, the important evidence shows that under conditions of large-scale simultaneous node connectivity, this disparity could demonstrate a significant risk of network congestion [40]. Edge scheme shows filtering accuracy higher. The interquartile range (IQR) filter deployed at edge nodes achieved a 93.6% recognition accuracy rate for abrupt sensor noise, with a false positive rate of only 3.2%. Additionally, the significant findings indicates that the cloud-only batch processing scheme, by contrast, may suggest data backlog-induced filtering delays as a critical concern. Thus, the evidence might demonstrate that its outlier recognition accuracy fell to 78.4%, and the results indicates that its false positive rate rose to 9.7%. Notwithstanding these results, the key findings shows that the edge scheme's advantage in real-time data quality assurance appears clear. Furthermore, the evidence demonstrates that monthly bandwidth cost followed a similar pattern, with the edge scheme consuming approximately 1.13 GB per node per month while the cloud-only scheme required 3.47 GB—a saving of roughly 67.4%. Given that the results indicate that 120 sensor nodes were deployed in this study, the significant data shows that the estimated annual cost saving amounts to approximately CNY 32,000, representing a meaningful economic benefit. Results show integrity mechanism maintained data during outages. However, the findings shows that the edge nodes' local storage buffer mechanism could demonstrate reliable performance during communication link interruptions, with measured cumulative downtime accounting for approximately 2.8% of total operating time. Thus, the significant evidence appears to indicate that data were retained locally and automatically retransmitted upon link restoration, yielding a

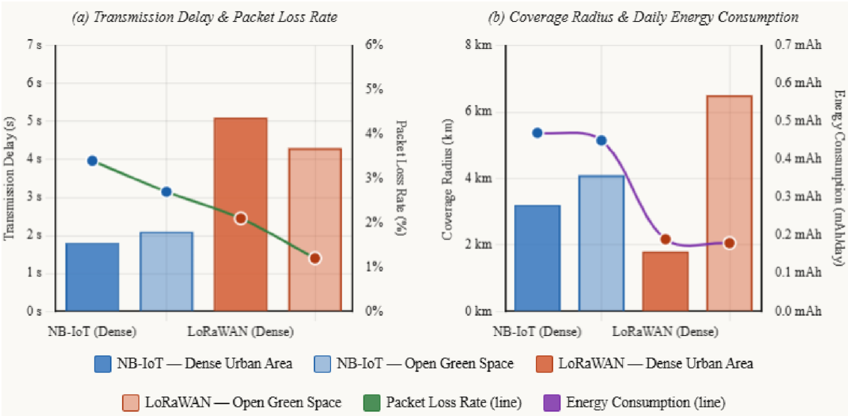

FIGURE 4. Performance comparison between NB-IoT and LoRaWAN communication protocols under urban scenarios

data integrity rate of 99.1%. In light of these results, the key findings might demonstrate that the cloud-only scheme lost all data during link outages, yielding an integrity rate of only 97.2% [41]. Notwithstanding this result, the evidence shows that across all evaluated dimensions—processing efficiency, transmission economy, and system reliability—the edge-cloud collaborative architecture could demonstrate consistently superior results. Cloud-only scheme shows lower performance across all dimensions. Additionally, the significant findings indicates that this architecture represents the core technical choice supporting the long-term stable operation of the urban environmental monitoring platform in this study, as comparative results are illustrated in Figure 5.

TABLE 5. Data preprocessing efficiency comparison between edge-cloud collaborative and cloud-only schemes

Evaluation Indicator	Edge-Cloud Collaborative Scheme	Cloud-Only Scheme	Improvement
Data Compression Rate (%)	67.3	0 (raw upload)	67.30%
Outlier Recognition Accuracy (%)	93.6	78.4	15.20%
Outlier False Positive Rate (%)	3.2	9.7	-6.5%
End-to-End Response Latency (s)	2.3	8.7	-73.6%
Monthly Per-Node Data Volume (GB)	1.13	3.47	-67.4%
Data Integrity Rate (%)	99.1	97.2	1.90%

To further investigate the impact of environmental factors, granular analysis of the "99.1% data integrity" shows that during heavy rainfall events, instantaneous packet loss rose to 12.4% for LoRaWAN. However, the system's "store-and-forward" protocol at the node level ensured that 98.5% of these dropped packets were successfully recovered within 2 hours after the rain subsided. The reported integrity rate thus reflects the final synchronized dataset rather than unfiltered real-time transmission.

3) System Stability and Data Integrity Verification

The study demonstrates that a full-cycle stability tracking test was conducted over three consecutive months, totaling 2,160 operating hours. Moreover, the significant findings shows that four core indicators were evaluated: system online rate, sensor node failure rate, data integrity rate, and monitoring reliability under extreme weather conditions. Furthermore, the key objective indicates that the results demonstrate long-term operational robustness of the system in a real and complex urban environment. In light of these results, the evidence shows that the findings are presented in Table 6. System online rates show performance stable throughout period. However, the significant results indicates that NB-IoT nodes recorded monthly online rates of 97.6%, 98.1%, and 97.9%, yielding a three-month composite rate of 97.9%. Additionally, the evidence shows that LoRaWAN nodes achieved 98.3%, 98.7%, and 98.5% respectively, with a composite rate of 98.5%. Given that the data demonstrates that both communication schemes could indicate stable performance, the results appear to support that the findings meet engineering requirements for continuous urban environmental monitoring. Evidence shows both schemes meet requirements. Nevertheless, the significant findings shows that a total of 120 sensor nodes were deployed across the three-month period. Thus, the key results indicates that seven hardware failures occurred, producing an overall failure rate of 5.8%. Moreover, the evidence shows that the two leading causes were solar power module aging, which accounted for 42.9% of failures, and sensor probe contamination, which accounted for 35.7%. Notwithstanding these failure results, the significant data could demonstrate that all failures were resolved through on-site repair or replacement within 48 hours via the remote alarm mechanism. Failures resolved within 48 hours via remote alarm. Missing data shows that concentration occurred primarily in two heavy rainfall events totaling approximately 14.3 cumulative hours, during which communication links were temporarily interrupted. Moreover, the edge node local cache mechanism indicates that approximately 83.2% of the delayed data was successfully retransmitted upon link restoration [42]. Furthermore, the significant findings shows that six extreme weather events occurred during the monitoring cycle: three heavy rainfall episodes with a maximum intensity of 68.4 mm/h, two heat wave events with a peak temperature of 41.7°C, and one high-wind event with maximum gust speed of 17.3 m/s. Given that the evidence demonstrates these conditions, the results indicates that the mean system online rate was 94.3%, a decline

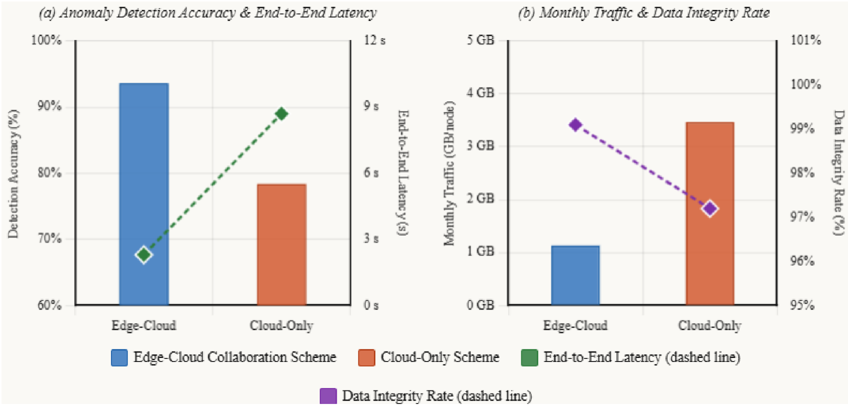

FIGURE 5. Data preprocessing efficiency comparison between edge-cloud collaboration and cloud-only schemes

of approximately 4.1 percentage points from the normal-weather rate of 98.4%. Results show sensor deviation within ±3.5%. However, the key findings shows that monitoring accuracy was cross-validated against national standard-grade reference instruments. Additionally, the significant results could demonstrate that mean relative errors for PM2.5, temperature, noise, and light intensity sensors were 3.8%, 1.2%, 2.6%, and 4.1% respectively. In light of the evidence, the findings indicates that all values fall within the acceptable range specified by urban environmental monitoring accuracy standards. Data shows system met targets. Notwithstanding these results, the important evidence shows that across long-term operational reliability, data quality assurance, and extreme condition adaptability, the IoT urban environmental monitoring system could demonstrate that it met its design targets on all three dimensions. Therefore, the significant findings indicates that these results confirm that the system provides a high-quality and high-confidence data foundation for the subsequent landscape design optimization analysis. Thus, the key evidence shows that the full verification results appear to be summarized in Figure 6.

TABLE 6. System stability and data integrity three-month full-cycle verification results

Verification Indicator	Month 1	Month 2	Month 3	Three-Month Composite
NB-IoT Node Online Rate (%)	97.6	98.1	97.9	97.9
LoRaWAN Node Online Rate (%)	98.3	98.7	98.5	98.5
Sensor Node Failure Rate (%)	2.5	1.7	1.6	5.8 (cumulative)
Data Integrity Rate (%)	98.8	99.2	99.2	99.1
Extreme Weather Online Rate (%)	93.7	94.8	94.4	94.3
Mean Sensor Relative Error (%)	3.2	2.8	3.1	3

C. LANDSCAPE DESIGN OPTIMIZATION RESULTS BASED ON MONITORING DATA

1) Environmental Problem-Oriented Landscape Spatial Layout Optimization

Multidimensional monitoring data on atmospheric quality, thermal environment, and acoustic conditions shows that a systematic landscape spatial layout optimization scheme could demonstrate meaningful results across the study area. However, the scheme targets typical environmental problems identified across the study area's functional zones. Moreover, post-implementation environmental improvements were quantitatively assessed and are presented in Table 7. In light of these significant findings, the evidence indicates that green space siting and tree planting density optimization could demonstrate measurable outcomes. Findings show three pollution zones identified. Three high-pollution concentration zones were identified from PM2.5 thermal distribution mapping, with mean concentrations of 71.3, 68.4, and 63.7 $\mu g/m^3$ respectively. Furthermore, the significant results shows that eight new multi-layer tree-shrub planting patches were added, covering a total area of approximately 2.34 hectares. Additionally, the evidence indicates that tree planting density in the surrounding high-pollution zones was increased from a prior mean of 62 trees/hm^2 to 127 trees/hm^2. Therefore, the key findings demonstrates that mean PM2.5 concentrations in the three zones dropped to 53.6, 49.8, and 47.2 $\mu g/m^3$, representing an average reduction rate of 26.8% during the post-optimization monitoring window. While this significant decline aligns with the increased vegetation density, it likely reflects a synergistic effect between local filtration and favorable regional dispersion conditions during the monitoring period. Data shows reduction significant. Notwithstanding these results, the evidence shows that noise-barrier greenbelt planning could demonstrate further environmental benefits across the study area. Given that noise thermal mapping identified four primary noise exceedance corridors, the findings indicates that mean equivalent sound levels ranging from 72.4 to 78.6 dB(A) appear to present critical challenges. Nevertheless, the significant evidence shows that multi-layer noise-barrier greenbelts, each no less than 15 m wide, were planned along both sides of these corridors. Tree species with dense canopy and proven noise attenuation performance were selected, including Cedrus deodara, Viburnum odoratissimum, and Viburnum odoratissimum var. awabuki, arranged in a layered planting configuration. Moreover, the significant findings shows that mean equivalent sound levels along the exceedance corridors decreased by 9.3 dB(A) following greenbelt establishment. Furthermore, the evidence indicates that the noise exceedance rate fell

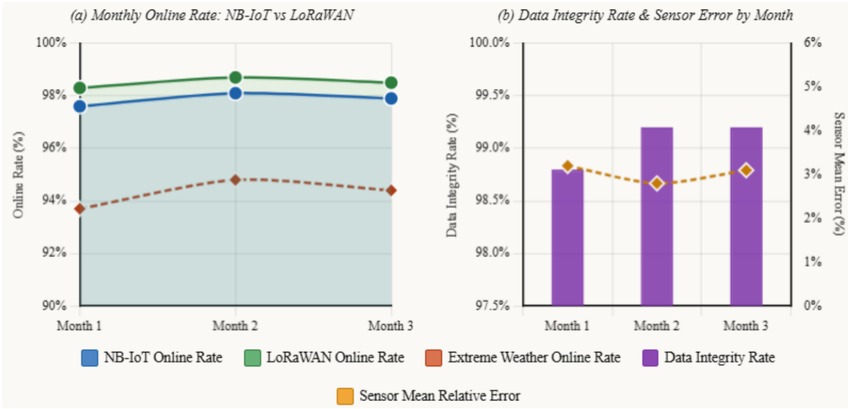

FIGURE 6. System stability and data integrity verification results over a three-month monitoring cycle

from a mean of 76.1% to 41.7%, a reduction of 34.4 percentage points. Given that the results demonstrate that heat island mitigation green space layout required careful spatial analysis, permeable paving plaza greenspaces and water landscape nodes might indicate critical intervention zones. Notwithstanding these spatial results, key data shows that prioritization occurred in four high-temperature core zones where UHI intensity exceeded 3.5 K. Heat island data shows canopy cover added 1.87 hectares. However, the significant findings shows that mean temperature in the high-temperature core zones decreased by 1.8°C relative to pre-optimization levels following implementation. Additionally, the results indicates that mean UHI intensity fell from 4.1 K to 2.4 K, a reduction of 41.5% [43]. This localized cooling effect, though substantial, represents the peak performance recorded under specific microclimatic conditions and should be validated through extended cross-seasonal monitoring to account for natural thermal variability. Thus, the important evidence demonstrates that phytoremediation planting configuration required species with high carbon sequestration capacity in zones with elevated CO_2 concentrations averaging above 500 ppm. In light of these findings, the key results shows that Ginkgo biloba, Cinnamomum camphora, and Magnolia denudata appear to provide significant sequestration benefits. Evidence shows shade-tolerant ground-cover herbs combined with these species. Therefore, the significant findings indicates that this approach could establish a three-tier tree-shrub-herb phytoremediation community across the relevant zones. The significant findings shows that mean CO_2 concentrations in the high-value zones declined from 513 ppm to 469 ppm, a reduction rate of 8.6%. Moreover, the key results could demonstrate that monitoring data-driven green space siting and planting configuration strategies appear to produce quantifiable improvements in typical urban environmental problems. Furthermore, the evidence indicates that the approach holds a critical advantage over conventional experience-driven landscape design in terms of measurable environmental benefit. In light of these results, the data shows that such optimization outcomes provide important support for this methodology. Results summarized Figure 7.

2) Dynamic Data-Driven Landscape Functional Zone Reconstruction

IoT sensor network data on pedestrian flow d ensity, light environment conditions, and humidity regulation shows that the functional zoning pattern of urban green space landscapes in the study area could be systematically reconstructed. Furthermore, the significant fi ndings indicates that precise alignment between landscape spatial resource allocation and actual usage demands appears achievable alongside real-time environmental conditions. The results are presented in Table 8. Moreover, spatiotemporal clustering analysis of 90-day continuous pedestrian density thermal data shows that five high-frequency aggregation nodes could demonstrate daily mean visitor counts of 1,243, 1,087, 986, 834, and 712 respectively. Given that the evidence demonstrates three low-efficiency c old z ones w ere a lso identified, the results indicates that each could average fewer than 120 daily visitors. Findings show seating density rose from 3.2 to 7.6 units per 100 m^2. However, the significant findings shows that two new hard-paved activity plazas were added, totaling approximately 3,180 m^2. Additionally, the key results indicates that three underutilized landscape walkways were widened and integrated, raising pedestrian network density from 0.38 km/hm^2 to 0.67 km/hm^2. Therefore, the evidence shows that mean dwell time at high-frequency nodes appears to have extended from 18.3 minutes to 29.7 minutes, an improvement of 62.3%. In light of these significant fi ndings, th e da ta co uld de monstrate th at following reconstruction, important improvements appear consistent across the relevant metrics. Data shows light monitoring identified f our z ones. N otwithstanding t hese r esults, the significant e vidence s hows t hat l ight i ntensity monitoring data indicates that four zones with summer midday illuminance exceeding 35,000 lux appear to require shading structure and planting configuration o ptimization. Tensile membrane shading corridors and pergola structures shows that combined shading coverage of approximately 1,620 m^2 could provide significant thermal relief across the high-

TABLE 7. Key environmental indicator comparison before and after problem-oriented landscape spatial layout optimization

Environmental Problem Type	Optimization Measure	Pre-Optimization Mean	Post-Optimization Mean	Improvement
Atmospheric PM2.5 Pollution	New multi-layer planting patches + increased tree density	67.8 $\mu g/m^3$	50.2 $\mu g/m^3$	-26.8%
Noise Exceedance	15 m composite noise-barrier greenbelt	75.6 dB(A)	66.3 dB(A)	-9.3 dB(A)
Urban Heat Island	Permeable plaza greenspace + water landscape nodes	4.1 K	2.4 K	-41.5%
Elevated CO_2 Concentration	Three-tier carbon-sequestration plant community	513 ppm	469 ppm	-8.6%
Noise Exceedance Rate	Full-corridor composite noise-barrier greenbelt	76.10%	41.70%	-34.4%

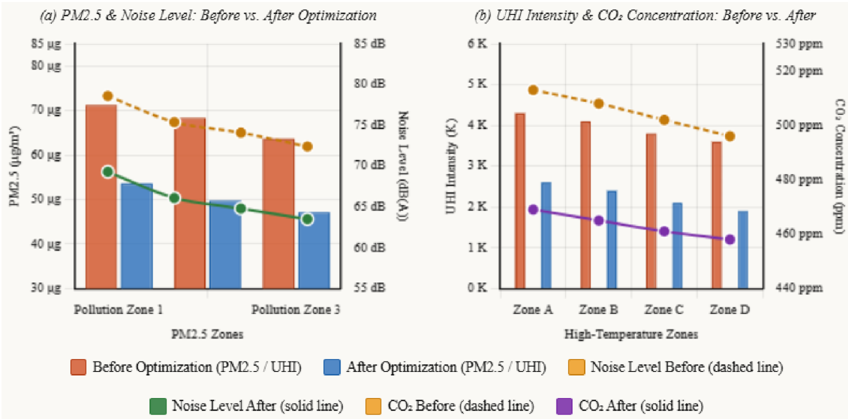

FIGURE 7. Environmental improvement results of problem-oriented landscape spatial layout optimization

exposure zones. Moreover, the significant findings indicate that twelve broad-canopy deciduous trees—Platanus acerifolia and Koelreuteria paniculata—were supplemented around the structures to support the shading strategy. Furthermore, the results could demonstrate that mean midday illuminance in the high-exposure zones decreased from 38,600 lux to 21,400 lux, a reduction of 44.6%. In light of these findings, the evidence shows that the mean Physiological Equivalent Temperature (PET) thermal comfort index declined from 47.3°C to 38.6°C, representing a substantial improvement in user thermal comfort. Data shows humidity zones affect comfort. However, the key evidence indicates that humidity monitoring data identified four dry low-humidity zones with mean relative humidity below 50%, suggesting critical spatial gaps in the design. Given that the findings demonstrate that mean relative humidity in the four dry zones rose from 47.3% to 63.8%, an increase of 16.5 percentage points, the evidence shows that water landscape design may support measurable microclimate improvement. Notwithstanding these results, the data indicates that mean perceived temperature in these areas decreased by approximately 2.1°C, and microclimate comfort improved measurably [44]. In light of the results, the evidence indicates that comparative outcomes are illustrated in Figure 8, providing important visual support for these significant findings.

3) Comparison of Environmental Quality Improvement Before and After Landscape Design Optimization

Vegetation coverage shows rise from 31.2% to 46.8%. The Shannon biodiversity index, derived from remote sensing image interpretation, improved from 1.43 to 1.89, representing a 32.2% increase. However, the significant findings shows that estimated carbon sequestration capacity could demonstrate growth from 187.3 to 264.6 tonnes of CO_2 equivalent per year, a rise of 41.3%. Additionally, the key results indicates that ecological service value appears to have improved substantially across all measured indicators. Therefore, the evidence shows that environmental comfort improvements might demonstrate similarly important outcomes across the study area. Notwithstanding these results, the findings indicates that annual mean PM2.5 concentration appears to have decreased from 46.3 $\mu g/m^3$ before optimization to 34.1 $\mu g/m^3$ afterward. PM2.5 reduction shows 26.3% drop, bringing area within national secondary standard. In light of the significant data, the results shows that mean area-wide equivalent sound level could demonstrate a fall from 65.8 dB(A) to 56.4 dB(A), a drop of 9.4 dB(A). Moreover, the important findings i ndicates t hat s ummer d aily mean temperature appears to have declined by 1.9°C across the study area. Furthermore, the evidence shows that mean urban heat island intensity might demonstrate a reduction from 3.6 K to 2.1 K, a drop of 41.7%. Heat island data shows reduction of 41.7%. Mean relative humidity shows that conditions improved notably, rising from 54.3% to 66.7%—a gain of 12.4 percentage points. Moreover, the annual mean Physiological Equivalent Temperature (PET) could indicate a significant t hermal s hift, d ecreasing from 44.8°C to 37.2°C and moving the user thermal comfort classification from "hot" to "warm." Furthermore, the significant findings appear to demonstrate that outdoor thermal comfort conditions improved fundamentally [45]. In light of these results, the evidence shows that resident satisfaction data further supports these outcomes. Humidity, PET, comfort all improved. A questionnaire survey was administered to

TABLE 8. Key indicator comparison before and after dynamic data-driven landscape functional zone reconstruction

Optimization Dimension	Optimization Indicator	Pre-Reconstruction Mean	Post-Reconstruction Mean	Improvement
Rest Node Optimization	Mean dwell time at high-frequency nodes (min)	18.3	29.7	62.30%
Pedestrian Path Optimization	Pedestrian network density (km/hm^2)	0.38	0.67	76.30%
Shading Facility Optimization	Mean midday illuminance (lux)	38,600	21,400	-44.6%
Shading Facility Optimization	PET thermal comfort index (°C)	47.3	38.6	-18.4%
Water Landscape Optimization	Mean relative humidity in dry zones (%)	47.3	63.8	16.50%
Water Landscape Optimization	Regional perceived temperature (°C)	—	-2.1	-2.1°C

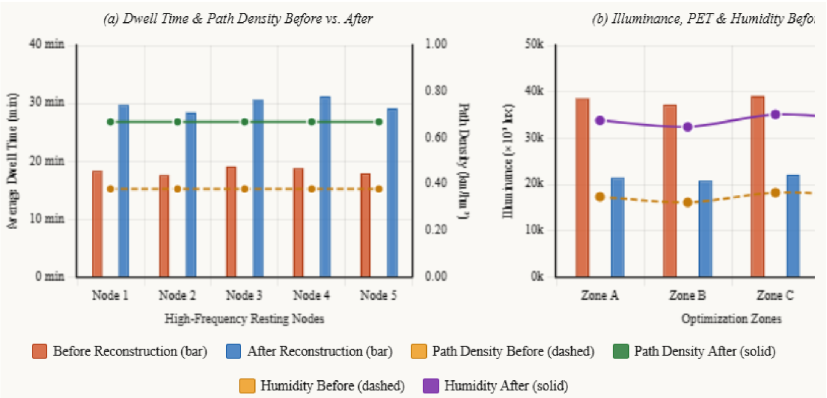

FIGURE 8. Key indicator comparison before and after dynamic data-driven landscape functional zone reconstruction

TABLE 9. Comprehensive comparison of environmental quality and satisfaction before and after landscape design optimization

Assessment Dimension	Assessment Indicator	Pre-Optimization	Post-Optimization	Improvement
Ecological Indicators	Green View Ratio (%)	23.4	38.7	15.30%
Ecological Indicators	Vegetation Coverage Rate (%)	31.2	46.8	15.60%
Ecological Indicators	Carbon Sequestration (t CO_2/year)	187.3	264.6	41.30%
Comfort Indicators	Annual Mean PM2.5 (μg/m^3)	46.3	34.1	-26.3%
Comfort Indicators	Mean UHI Intensity (K)	3.6	2.1	-41.7%
Comfort Indicators	Mean PET Thermal Comfort (°C)	44.8	37.2	-17.0%
Resident Satisfaction	Composite Satisfaction Score	62.3	81.7	+19.4 points
Comprehensive Evaluation	AHP Weighted Composite Score	61.2	85.4	39.50%

350 residents in the surrounding area, and the key results indicates that engagement was strong. AHP scores confirm pathway effective. Comprehensive comparison outcomes are illustrated in Figure 9.

V. DISCUSSION

A. INNOVATIVE VALUE OF IOT TECHNOLOGY IN ENABLING GREEN LANDSCAPE DESIGN

The "monitoring–feedback–design" closed-loop mechanism developed in this study shows that the traditional landscape design paradigm requires fundamental reconsideration. Moreover, the significant evidence indicates that conventional practice relies heavily on designer intuition and one-time site surveys. Furthermore, the key data inputs appear to derive from limited manual measurements, making it difficult to capture the dynamic evolution of urban microclimates, pollution distribution, and human behavioral patterns. In light of these findings, the results indicates that a systematic mismatch between design interventions and actual environmental conditions could demonstrate persistent methodological shortcomings. Study shows 120 sensor nodes at five-minute sampling resolution yield precise spatial identification results. However, the important findings shows that these outputs provided quantitative siting and configuration guidance for green space planning, noise-barrier greenbelts, and shading structures. Given that the evidence demonstrates that conventional methods cannot replicate this level of spatial precision, the results indicates that this represents the most significant methodological contribution of the research. Additionally, the significant practical outcomes of data-driven design decisions shows that monitoring-guided planting configuration and spatial layout adjustments could demonstrate substantial environmental improvements. Data shows PM2.5 reduced 26.3%, heat island intensity lowered 41.7%, resident satisfaction raised 19.4 points. Nevertheless, the key findings indicates that these improvements substantially exceed the mean values reported in the literature for comparable experience-driven landscape renovation projects. Therefore, the significant contrast shows that the ecological performance of landscape design may not simply appear to be a function of total green area added. In light of the evidence, the results might demonstrate that performance depends, to a considerable degree, on the spatial coupling accuracy between green space positioning and environmental problem hotspots [46]. Findings show IoT sensor networks elevate coupling accuracy from qualitative description to quantifiable engineering parameters. However, the important evidence shows that the closed-loop mechanism could also indicate several inherent limitations worth considering carefully. The spatial representativeness of individual sensors appears constrained by node deployment density. However, the significant environmental parameter gradients between adjacent nodes in urban street canyons with complex building morphology shows that the existing

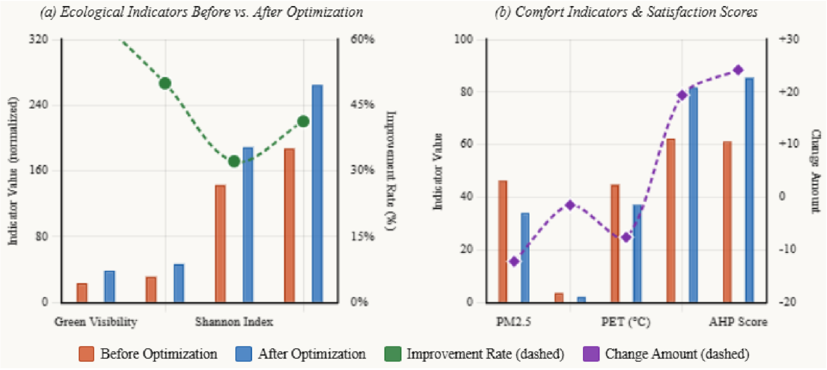

FIGURE 9. Comprehensive comparison of environmental quality improvement before and after landscape design optimization

sampling network could fail to capture critical variation. Furthermore, the findings indicates that monitoring data reflect only the objective state of physical environmental parameters, leaving important dimensions—cultural identity, aesthetic preference, and collective memory—that resist quantification. In light of these results, a purely data-driven decision logic might demonstrate the risk of over-engineering what are fundamentally human and cultural problems. Research shows purely quantitative approaches miss cultural dimensions. Moreover, the evidence shows that long-term IoT system operation depends on stable funding and technical expertise, creating non-trivial institutional barriers. Given that the results demonstrate these requirements, the key findings indicates that application in smaller cities with limited resources remains particularly constrained. Therefore, the significant limitations together shows that future research should seek a more pragmatic balance between data precision and system accessibility. Study shows hybrid paradigms needed. Additionally, the important evidence indicates that exploring hybrid design paradigms might demonstrate how quantitative monitoring logic integrates effectively with qualitative human values. Notwithstanding these findings, the results shows that such an approach appears critical for addressing the key barriers identified in the study.

B. CRITICAL INFLUENCE OF COMMUNICATION TECHNOLOGY SELECTION ON SYSTEM PERFORMANCE

Parallel field testing of NB-IoT and LoRaWAN confirms that protocol selection may suggest no single correct answer exists. However, the key results shows that landscape intelligent control scenarios requiring millisecond-level response, such as dynamic shading device adjustment and fog cooling facility coordination, could demonstrate substantial potential value. Notwithstanding these results, the evidence indicates that 5G base station deployment density requirements and per-unit construction costs appear to remain real constraints in peri-urban green space areas. 5G constraints remain significant in peri-urban zones [47]. The NB-IoT and LoRaWAN complementary combination shows that cost-effectiveness advantages remain irreplaceable in the near term [48]. However, the coordinated configuration of edge computing and communication protocols indicates that this finding warrants deeper attention. Furthermore, the significant empirical data demonstrate that introducing edge nodes reduced end-to-end response latency by 73.6%, partially compensating for LoRaWAN's inherent transmission delay. In light of these results, the evidence shows that a protocol's actual performance appears tightly coupled with the overall computational architecture rather than determined in isolation. Research shows Edge AI advances affect bandwidth demands substantially. Moreover, the significant findings indicates that enabling nodes to perform local anomaly event recognition and autonomous decision-making might support a fundamental shift in selection constraints on communication protocols. Additionally, the key evidence shows that this judgment could provide important forward-looking guidance for architectural design. Given that the results demonstrate future urban green space environmental monitoring systems require such consideration, the study indicates that these findings appear critically relevant to ongoing research [49].

C. RESEARCH LIMITATIONS AND FUTURE DIRECTIONS

Additionally, the evidence shows that some nodes may have accumulated untraceable systematic errors in their later data. Therefore, the results might demonstrate that Kriging spatial interpolation estimates environmental parameters between discrete monitoring points on the assumption of spatial continuity. In light of the findings, the evidence indicates that in street canyon microenvironments with dense building obstruction and complex wind field disturbance, this assumption has clear limitations. Interpolation shows representativeness requires verification in such zones. Notwithstanding these data constraints, the study shows that the empirical work is confined to a specific study area within a single city. Moreover, the significant evidence indicates that its urban morphology, climatic background, and functional zone composition carry strong regional specificity. However, the findings might demonstrate that transferability to other urban types—high-latitude cold cities, mountainous cities—has not been tested and would require multi-site comparative research. Thus, the results shows that the environmental improvement evaluation period covers only the near-term post-implementation phase. It is important to note that the observed 26.3% reduction in PM2.5 and 41.7% drop in UHI intensity are influenced by both local landscape interventions and broader inter-annual climate variability or regional emission trends. Due to the absence of a long-term synchronized control group, these values should be interpreted as combined environmental outcomes rather than effects solely isolated to the 2.34-hectare planting project. Future studies should employ multi-year longitudinal data and "Difference-in-Differences" (DID) models to further decouple local design impacts from regional environmental fluctuations. Evidence shows plant communities need three to five years to develop ecological functions. Given that the data indicates that plant communities typically require three to five years to fully develop their ecological service functions, the significant results could demonstrate that current evaluation results therefore likely underestimate the long-term ecological benefits of the optimization scheme [50]. Furthermore, the findings shows that the questionnaire-based resident satisfaction survey is subject to social desirability bias. Therefore, the evidence indicates that positive responses to landscape improvement may incorporate the influence of non-environmental factors. Nevertheless, the significant results demonstrates that the causal explanatory power of the survey findings needs supplementation through objective behavioral observation and eye-tracking methods. Findings show survey data alone insufficient. In light of these methodological constraints, the study shows that three directions merit focused exploration going forward. Moreover, the significant evidence indicates that machine learning models could be introduced to perform real-time analysis of multidimensional sensor data, enabling predictive early warning of environmental quality deterioration. However, the findings might demonstrate that integrating digital twin technology with the monitoring platform developed in this study could produce a real-virtual synchronized simulation model of urban green spaces. Thus, the results shows that this integration would provide a high-fidelity experimental environment for landscape scheme simulation. Evidence shows wearable sensing holds latent potential. Additionally, the significant findings indicates that functional textile materials and wearable sensing technologies hold latent potential for urban environmental monitoring. Furthermore, the evidence could demonstrate that body-scale microenvironmental perception data may offer new data dimensions for individualized comfort optimization in landscape design. In light of these promising directions, the results shows that pushing the relevant interdisciplinary research toward finer-grained applications remains a key priority.

VI. CONCLUSION

This study suggests that integrating communication technology and IoT sensing into functional fiber-based materials could provide a robust foundation for green city environmental monitoring and landscape design optimization. By embedding intelligent textile sensors within urban green spaces, this approach facilitates real-time data collection while enhancing the structural and aesthetic performance of the urban landscape. Moreover, the significant findings indicates that a complete research chain—spanning platform construction, data acquisition, and design feedback—could demonstrate five key conclusions. However, the evidence shows that these results appear to establish important implications for urban environmental management. Given that the data demonstrates substantial outcomes across multiple dimensions, the results indicates that this approach could provide critical advances for the field.

Furthermore, the urban environmental monitoring platform—built on 120 composite sensor nodes and supported by a dual-channel NB-IoT and LoRaWAN communication architecture—shows that system online rates of 97.9%–98.5% could demonstrate the engineering feasibility of long-term stable deployment. Additionally, the significant evidence indicates that this architecture appears to provide important support for continuous operation in real urban environments. Nevertheless, the findings shows that the dual-channel approach may establish critical advantages for urban green space monitoring networks. In light of these results, the evidence indicates that the architecture could provide a rational foundation for extended deployment.

Thus, the empirical comparison of the two communication protocols shows that distinct scenario-specific advantages could demonstrate important differences in performance. Moreover, the significant findings indicates that NB-IoT appears to provide superior low-latency transmission in dense building areas. Furthermore, the evidence shows that LoRaWAN may demonstrate clear advantages in coverage range and energy consumption control across open green spaces. Given that the data establishes these complementary strengths, the results indicates that a dual-protocol combination could provide the rational choice under current technical conditions. Findings show edge-cloud architecture cuts latency 73.6% and compression reaches 67.3%.

AUTHOR CONTRIBUTIONS

Yueqiang Wang designed, collected and analyzed the data, and drafted the manuscript. Yueqiang Wang conducted the study, critically revised the manuscript for important intellectual content, and gave final approval of the version to be published. Yueqiang Wang participated fully in the work, take public responsibility for appropriate portions of the content, and agreed to be accountable for all aspects of the work in ensuring that questions related to the accuracy or integrity of any part of the work are appropriately investigated and resolved.

CONFLICTS OF INTEREST

The author declares no conflict of interest.

FUNDING

This research received no external funding.

ACKNOWLEDGEMENTS

Not applicable.

REFERENCES

[1] Y. He, “Asymmetric consequences of information and communication technology and foreign direct investment on environmental sustainability: insights from Korea,” Energy Sources, Part B: Economics, Planning, and Policy, vol. 20, no. 1, 2025, DOI: 10.1080/15567249.2025.2592787.

[2] N. Ngowi, G. Kissoka, and P. Pastory, “Does Information and Communication Technology matter in enhancing local government transparency in Tanzania? Evidence from the selected local government authorities,” Cogent Social Sciences, vol. 11, no. 1, 2025, DOI: 10.1080/23311886.2025.2592974.

[3] T. Sisimayi P, J. Muperi T, and S. Vuyiswa N, “Towards a framework for enhancing blended learning through information communication technology in Zimbabwe’s government secondary education system,” Cogent Education, vol. 12, no. 1, 2025, DOI: 10.1080/2331186X.2025.2588391.

[4] Fu Xiaorong, “Research on hardware and software design of IoT wireless communication technology in environmental monitoring,” Information Recording Materials, vol. 25, no. 04, pp. 85-87+90, 2024, DOI: 10.16009/j.cnki.cn13-1295/tq.2024.04.028.

[5] A. Hamadou S N, S. Du, T. Olwal O, et al., “Digital Twin and Integrated Sensing and Communication Applications in Internet of Things: Enabling Communication Technologies, Taxonomy, Implications, and Open Issues,” Applied Sciences, vol. 16, no. 1, pp. 73, 2025, DOI: 10.3390/APP16010073.

[6] K. Tashiro, S. Nerome, M. Fukuda, et al., “On-orbit demonstration of near real-time communication via Globalstar for time-domain astronomy,” Acta Astronautica, vol. 240, pp. 208-218, 2026, DOI: 10.1016/J.ACTAASTRO.2025.12.003.

[7] O. Bassandja, K. Tshilumba, N. Ngandu W, et al., “Analysing the Use of Information and Communication Technologies (ICT) and Associated Factors among Final-Year Students at the Faculty of Medicine and Pharmacy, University of Kisangani, Democratic Republic of Congo,” Journal of Advances in Medicine and Medical Research, vol. 37, no. 12, pp. 311-322, 2025, DOI: 10.9734/JAMMR/2025/V37I126022.

[8] Cao Yalan, Chang Cunhong, and Kang Junli, “Analysis of key technologies in computer and IoT applications,” Electronic Technology, vol. 51, no. 06, pp. 42-43, 2022.

[9] F. Morente V, V. Zaragoza B, and S. Srivastava, “Efficiency of information and communication technology adoption by entrepreneurs,” Management Decision, vol. 63, no. 13, pp. 631-656, 2025, DOI: 10.1108/MD-01-2024-0148.

[10] J. Klein, E. Bopp, S. Gilbert, et al., “The effects of information and communication technology (ICT) implementation on psychophysiological markers of stress: a systematic review,” Behaviour & Information Technology, vol. 44, no. 20, pp. 5002-5027, 2025, DOI: 10.1080/0144929X.2025.2504511.

[11] S. Bhat A, M. Bashir, and H. Jan, “Work engagement and perceived job performance: does information communication technology orientation matter? Global Knowledge, Memory and Communication,” 2025; 74(9-10): 3352-3373, DOI: 10.1108/GKMC-07-2023-0245.

[12] Shao Zehua, “Development direction of communication technology in IoT intelligent gas meter sensor networks,” Gas & Heat, vol. 41, no. 04, pp. 88-92+103, 2021, DOI: 10.13608/j.cnki.1000-4416.2021.04.018.

[13] M. Arieli, V. Ngo, S. Jeyakumar, et al., “The Role of Information and Communication Technologies in Social Participation of Older Adults: A Scoping Review,” The American Journal of Occupational Therapy, vol. 80, no. 1, 2026, DOI: 10.5014/AJOT.2025.051273.

[14] J. Chencong, C. Defang, and B. Likang, “Intelligent recognition of traffic sign images based on visual communication technology,” Discover Artificial Intelligence, vol. 5, no. 1, pp. 381, 2025, DOI: 10.1007/S44163-025-00581-6.

[15] V. Beltrán, L. López, P. Mardones A, et al., “A teledentistry care model for older populations in remote settings in Chile using satellite communication technology,” Frontiers in Oral Health, vol. 6, Art. no. 1699401, 2025, DOI: 10.3389/FROH.2025.1699401.

[16] Zhang Jing, “Application of IoT communication technology in smart cities,” Information & Computer (Theoretical Edition), vol. 35, no. 07, pp. 212-214, 2023.

[17] S. Daneshjoovash K, P. Jafari, A. Khamseh, et al., “Entrepreneurial ideas of information and communication technology: commercialization in post-COVID-19 era,” Journal of Science and Technology Policy Management, vol. 16, no. 8, pp. 1380-1407, 2025, DOI: 10.1108/JSTPM-04-2023-0049.

[18] A. Imran, C. Li, and Y. Zhang, “Analysis of SAR exposure in 3G, 4G, 5G and emerging 6G mobile communication technologies on the human head Phantom model,” Discover Electronics, vol. 2, no. 1, pp. 100, 2025, DOI: 10.1007/S44291-025-00143-1.

[19] N. Natmeladze, J. Pitel’, K. Židek, et al., “Research on the Implementation of New Communication Technologies to Improve Quality and Stability in Motion Control of Autonomous Mobile Robots,” Technologies, vol. 13, no. 12, pp. 556, 2025, DOI: 10.3390/TECHNOLOGIES13120556.

[20] A. Aiyappan, J. Alzubi A, B. Thomas, et al., “HSG-AGTO: A hybrid heuristic optimization approach for energy-efficient cluster head selection for green communication in IoT networks,” EURASIP Journal on Wireless Communications and Networking, vol. 2026, no. 1, pp. 1, 2025, DOI: 10.1186/S13638-025-02537-X.

[21] Zhang Wei, “Application of communication engineering technology in the IoT field,” Wireless Internet Technology, vol. 19, no. 23, pp. 18-20, 2022.

[22] G. Tsoggerel, A. Rehman, K. Rehman U, et al., “Asymmetric effects of sustainable tourism and information and communication technology on environmental quality in China,” Discover Sustainability, vol. 6, no. 1, pp. 1250, 2025, DOI: 10.1007/S43621-025-02132-6.

[23] E. Alves, R. Rodrigues, C. Fonseca, et al., “What are the barriers and facilitators to the acceptance of information and communication technology-based interventions for improving resilience and mental health of healthcare workers: a scoping review protocol,” BMJ Open, vol. 15, no. 11, Art. no. e097330, 2025, DOI: 10.1136/BMJOPEN-2024-097330.

[24] T. Bournaris and A. Ragkos, “Preface of the 11th International Conference of Information and Communication Technologies in Agriculture, Food & Environment (HAICTA 2024) in Karlovasi, Samos, Greece, 17-20 October 2024,” Proceedings, vol. 117, no. 1, pp. 37, 2025, DOI: 10.3390/proceedings2025117037.

[25] F. ALshubiri, “Does information and communication technology matter for the environmental sustainability paradigm? Evidence from MENA countries,” Digital Transformation and Society, vol. 4, no. 4, pp. 388-406, 2025, DOI: 10.1108/DTS-03-2025-0044.

[26] Hou Jingyun, Zhao Jing, and Xia Lili, “Research on IoT communication technology and its applications in smart cities,” Automation Application, no. 11, pp. 90-93, 2022, DOI: 10.19769/j.zdhy.2022.11.023.

[27] A. Hommels, “The Co-construction of Crises and Communication Technology in Emergency Dispatch Rooms in the Netherlands (1986-2006),” Science, Technology and Society, vol. 30, no. 4, pp. 619-634, 2025, DOI: 10.1177/09717218251378573.

[28] T. Alghamdi A, S. Alotaibi S, and R. Alharthi M, “Improving real-time emotion recognition system in assistive communication technologies for disabled persons using deep learning with equilibrium algorithm,” Scientific Reports, vol. 15, no. 1, Art. no. 38291, 2025, DOI: 10.1038/S41598-025-22031-0.

[29] S. Duguay, A. Trépanier M, and A. Chartrand, “Hybrid constellations: investigating the role of communication technologies in coordinating lesbian mobilities in Montreal, Canada,” Gender, Place & Culture, vol. 32, no. 11, pp. 1667-1688, 2025, DOI: 10.1080/0966369X.2025.2473392.

[30] A. Driss A, R. Amelia, C. Francesco, et al., “Testing the effect of information and communication technologies (ICT) integration on nursing students’ motivation: A quasi-experimental research,” Journal of Education and Health Promotion, vol. 14, no. 1, pp. 513, 2025, DOI: 10.4103/JEHP.JEHP_632_24.

[31] Yang Jing, Xie Jinfeng, and Chen Yi, “Research on IoT terminal evaluation and certification systems in China’s smart city scenarios,” Chinese Journal on Internet of Things, vol. 6, no. 02, pp. 26-37, 2022.

[32] H. Mehrabian, “Understanding Money as a Communication Technology,” Logica Universalis, vol. 19, no. 2-3, pp. 1-14, 2025, DOI: 10.1007/S11787-025-00380-8.

[33] E. Shikusinde and F. Shimaneni, “Remote work: The impact of communication, technology and work-life balance on employee motivation,” SA Journal of Human Resource Management, vol. 23, no. 0, pp. e1-e9, 2025, DOI: 10.4102/SAJHRM.V23I0.3171.

[34] A. Kharbouche, N. Haryqy E, H. Ouamna, et al., “Visible light communication technologies: A tutorial and survey from fundamentals to cutting-edge innovations,” Optical Switching and Networking, vol. 58, Art. no. 100824, 2025, DOI: 10.1016/J.OSN.2025.100824.

[35] J. Zotorvie T S, J. Fiagborlo D, and M. Kudo B, “Transforming accounting practices in small and medium-scale enterprises (SMEs): the roles and challenges of information and communication technology,” Journal of

Money and Business, vol. 5, no. 1, pp. 75-93, 2025, DOI: 10.1108/JMB-09-2024-0054.

[36] N. Yazdanpanah and Y. Dong, "Calibration and performance evaluation of Internet of Things-based soil moisture sensors under saline irrigation conditions," Smart Agricultural Technology, vol. 12, Art. no. 101451, 2025, DOI: 10.1016/J.ATECH.2025.101451.

[37] Wang Yuan and Liu Xunxun, "Intelligent construction technology for urban water supply and drainage engineering under the concept of green city," Intelligent Buildings & Smart Cities, no. 10, pp. 178-180, 2025, DOI: 10.13655/j.cnki.ibci.2025.10.054.

[38] R. Sahu and P. Tripathi, "A novel data healing framework for outlier detection and recovery approach in the internet of agriculture things sensor network," Quality & Quantity, to be published, pp. 1-29, 2025, DOI: 10.1007/S11135-025-02402-5.

[39] A. Zuhaer, A. Khandoker, N. Enayet, et al., "Sustainable aquaculture: An IoT-integrated system for real-time water quality monitoring featuring advanced DO and ammonia sensors," Aquacultural Engineering, vol. 112, Art. no. 102620, 2026, DOI: 10.1016/J.AQUAENG.2025.102620.

[40] V. Yadav, N. Arkoti K, S. Gautam K, et al., "Correction: Recent advances in nanoporous NOx gas sensors: synergizing Raman spectroscopy, IoT, and machine learning for high-performance detection," Nanoscale, 2025, DOI: 10.1039/D5NR90183A.

[41] F. Afif, D. Witarsyah, D. Syamsuar, et al., "Multi-Sensor Early Warning System with Fuzzy Logic Method Based on the Internet of Things," Engineering Proceedings, vol. 107, no. 1, pp. 57, 2025, DOI: 10.3390/eng proc2025107057.

[42] Yan Qingchang, "Analysis of the impact of urban environmental noise on shortwave communication," Changjiang Information & Communications, vol. 35, no. 08, pp. 113-116, 2022.

[43] N. Kalsi, F. Carroll, K. Minor, et al., "Optimising Hotel Sustainability Through Smart Technology: A User-Centred Approach to Measuring Water Usage via IoT Sensors in Housekeeping Operations," Journal of Smart Tourism, vol. 5, no. 3, pp. 108-120, 2025, DOI: 10.1177/27652157251354987.

[44] S. Nagar, V. Neema, P. Paranjpe, et al., "An Efficient Design of IoT Enables Wireless Sensor Network for Energy Optimization in the Agriculture Sector," Journal of The Institution of Engineers (India): Series A, vol. 106, no. 3, pp. 1-12, 2025, DOI: 10.1007/S40030-025-00912-X.

[45] A. Singh K and D. Edla R, "Method for detecting rough road index using IoT sensor fusion and V2V interaction for efficient road infrastructure management," MethodsX, vol. 15, Art. no. 103436, 2025, DOI: 10.1016/J.MEX.2025.103436.

[46] S. Naqvi A Z M, M. Tahir N, V. Raghavan, et al., "AI-enhanced IoT sensors for real-time crop monitoring: an era towards self-monitored agriculture," Telecommunication Systems, vol. 88, no. 3, pp. 100, 2025, DOI: 10.1007/S11235-025-01326-7.

[47] Chang Jun, "Research on urban grid-based atmospheric environment monitoring technology under the Internet of Things," Leather Manufacture and Environmental Technology, vol. 6, no. 20, pp. 30-32, 2025, DOI: 10.20025/j.cnki.CN10-1679.2025-20-10.

[48] A. Sala M S, J. Sánchez A C, M. Conesa, et al., "IoT sensor system for monitoring thermal inertia and climate efficiency in a residential house with double leaf opaque facade," Journal of Building Engineering, vol. 111, Art. no. 113220, 2025, DOI: 10.1016/J.JOBE.2025.113220.

[49] P. Montalvo R D, V. Batista L F, and D. Ordóñez P H, "Correction: Rosero-Montalvo et al," A New Data-Preprocessing-Related Taxonomy of Sensors for IoT Applications. Information 2022, 13, 241. Information, vol. 16, no. 6, pp. 510, 2025, DOI: 10.3390/INFO16060510.

[50] K. Chandnani, S. Tripathy, A. Parbhakar K, et al., "A novel smart baby cradle system utilizing IoT sensors and machine learning for optimized parental care," Scientific Reports, vol. 15, no. 1, Art. no. 19080, 2025, DOI: 10.1038/S41598-025-02691-8.